



Modelling of Fuel Rod Hydriding Failures in Water Reactors

Afanasieva E.Yu., Evdokimov I.A., Khoruzhii O.V., Likhanskii V.V., Sorokin A.A.

State Research Center of the Russian Federation, Troitsk Institute for Innovation and Fusion Research
(SRC RF TRINITI), Troitsk, Moscow reg., Russia

ABSTRACT

Hydriding phenomena in zirconium claddings may cause both the primary and secondary fuel rod failures at operating nuclear power plants (NPPs). The main sources of hydrogen leading to typical primary defects are organic impurities or residual moisture in fuel which are trapped inside fuel rod during the manufacturing process. After the primary defect is formed steam accumulation in fuel element may lead to formation of the secondary defect and a serious rod failure. For purposes of fuel management it is important to have an instrument that allows to determine the causes of each hydriding failure, to assess the possibility of hydriding failures in rods with different parameters under various operation conditions, to predict the behavior of defective fuel rods and the release of activity into coolant. Nowadays a worldwide approach to solve such problems is to develop mechanistic codes which provide a self-consistent modelling of physical and chemical processes in operating fuel rods [1-3].

The present paper reports on mechanistic models which were developed to describe primary hydriding phenomena in claddings of initially intact rods with residual moisture. The models include the following key processes: fuel rod thermal behavior, UO₂ fuel oxidation in steam-hydrogen atmosphere under irradiation, hydrogen diffusion in zirconium and in the hydride, growth of the hydride phase. Fuel rod thermomechanical behavior is calculated with an integral fuel code RTOP. An oxidation model represents the effects of temperature dynamics and temperature profile along fuel axis and radius on fuel oxidation as well as on hydrogen accumulation inside the fuel rod. Along with ordinary thermal dissociation of H₂O molecules the oxidation model also deals with radiolysis of steam-hydrogen mixture due to fission fragments. The present radiolysis model takes into account the effects of gas mixture composition, temperature and pressure. A new model of cladding hydriding is proposed in which calculation of the massive hydride growth is performed in 2-D geometry. Hydrogen transport in zirconium cladding is modeled with account for thermodiffusion.

The RTOP code comprising the developed models allows to calculate different scenarios of hydriding rod failures under given operation conditions. Test calculations were carried out and compared to available data. It is shown that there are threshold values of initial steam content inside the intact fuel rod which lead to possibility of through-cladding hydride growth and formation of the primary defect. These threshold values depend on oxidation state of cladding inner surface, linear power profile in the fuel rod, fuel rod geometry, cladding temperature conditions and hydrogen diffusivities in zirconium and zirconium hydride.

KEY WORDS: nuclear water reactor, fuel rod, zirconium cladding, primary and secondary failure, defective rod, hydrogen generation, massive hydride, radiolysis, steam-hydrogen mixture, fuel oxidation, fuel stoichiometry.

INTRODUCTION

Fuel rod failures at operating NPPs accompanied by release of activity into coolant are repeatedly reported in literature. If activity levels monitored at an NPP exceed specified limits a reactor facility is to be shut down and high-cost measures are invoked to locate failed fuel bundles in a pile. At present time much attention is drawn to problems of defective fuel since a tendency to long-term fuel cycles and increase in fuel burnup result in degradation of cladding properties and higher risks of rod damage.

Formation of primary defects in cladding is generally attributed to manufacturing defects, to process of fretting corrosion (in presence of rubbing areas on cladding), to nodular corrosion, to impact of extraneous particles on cladding (“debris” particles), to pellet-cladding interactions [4,5]. According to [6], the major failure cause in BWRs and also the common cause in PWRs since 1968 till 1977 was the local growth of primary massive hydrides. Over the last years the total number of fuel rod failures has steadily decreased for BWRs and PWRs, but a certain population of primary defects is still related to massive hydriding [7].

Massive cladding hydriding is possible in presence of redundant hydrogen impurities inside fuel rod. The main source of hydrogen in the BWR and PWR fuel rods failed over 1968-1977 was residual moisture in the UO₂ pellets. That was a result from a non-optimized manufacturing process [6].

The general sequence of events in the initially intact rod with residual moisture is as follows. While fuel rod is put to operation for the first time, fuel temperature is increased, available moisture flashes into steam and fills the gas volume inside the fuel rod. Hydrogen produced due to dissociation and radiolysis of steam is efficiently taken up by the cladding. Generally this process is hindered by an oxide film over cladding inner surface. Some factors are known

which cause crippling of the oxide. Among them, for instance, are pellet-cladding mechanical interaction (PCI) or dissolution of the oxide film when hydrogen content in the gas phase exceeds a certain threshold level [8]. After the oxide layer is locally off, rapid penetration of gaseous hydrogen into metal starts in this location. Hydrogen concentration in near-surface region is increased and for high partial pressure of H₂ may exceed the solubility limit in zirconium at local temperature. In this case massive hydride will grow on cladding inner surface (so-called “blister” or “sunburst”).

This paper presents a set of physical models been developed to describe the blister initiation and growth in zirconium cladding. The following physical processes are included into modelling:

- radiolysis of steam-hydrogen mixture by fission fragments;
- fuel oxidation and hydrogen generation with account for radiolysis;
- gradual hydrogen penetration into cladding through the oxide layer on its inner surface;
- local hydrogen adsorption by cladding where the oxide layer is damaged or dissolved;
- precipitation of hydride phase when hydrogen terminal solubility in zirconium is reached;
- hydrogen 2-D diffusive transport in cladding with account for thermodiffusion and for dynamics of diffusion field in the vicinity of the moving hydride front;
- growth of the massive hydride with due regard of microcracking of hydride layers.

Listed processes are combined in two major models which are discussed in detail below. Incorporated into the integral RTOP code [9], these models enable to evaluate possibility and typical times for blisters to grow through the cladding wall depending on initial parameters (moisture content, rod linear power, permeability of the oxide layer). This provide an opportunity to calculate different scenarios of hydriding rod failures under given operation conditions.

MODEL FOR RADIOLYSIS OF STEAM-HYDROGEN MIXTURES AND IN-PILE FUEL OXIDATION

Hydrogen inside a fuel rod with residual moisture is generated mainly due to oxidation of UO₂ fuel (along with cladding oxidation) in steam. The overall reaction can be expressed by single equation



It is speculated that steam radiolysis by fission fragments may produce a substantial accelerating effect on fuel oxidation under in-pile conditions [10,11]. Fission fragments induce decomposition of H₂O molecules into a lot of intermediate products: ions, electrons, excited atoms, radicals. Active interreaction of intermediate particles eventually results in formation of molecular hydrogen and hydrogen peroxide. Because of its high chemical activity, peroxide is an efficient fuel oxidant



Hence, radiolysis affect the major processes that govern hydrogen accumulation inside the fuel rod. A model for primary hydriding in the operating rod should adequately take this influence into account. First of all, the available fuel oxidation models are to be revised. Based on the laboratory tests these models may underestimate in-pile fuel oxidation rates as they do not include effects of radiolysis.

Note, that the problem is of essentially nonlocal nature. Many of basic parameters are functions of axial and radial position in the fuel rod. This fact necessitates to model the distributed system. The below model for calculation of hydrogen source inside operating rod due to fuel oxidation includes dependences on pressure and accounts for inhomogeneities of temperature, gas mixture composition and irradiation conditions over the rod. It also accounts for changes in gas mixture composition in processes of fuel oxidation and hydrogen uptake by cladding.

Radiolysis of Steam-Hydrogen Mixture

The model is based on available literature data on radiolysis of pure steam, pure hydrogen and gas systems [10,12,13]. In low-density gas mixtures radiation decomposition of each component may be regarded independently. Low-density conditions are typical for steam-hydrogen atmosphere inside intact rods and as first approximation are valid for defective rods operating in PWRs and BWRs. After rapid recombination of intermediate particles within fission fragment tracks, radiation chemistry of steam-hydrogen mixture may be roughly reduced to interaction of radicals H, OH and molecules H₂O, H₂, H₂O₂ [12,13]:



Rates of these chemical reactions are chosen according to [14]. Radicals are born in proportion to their radiation yields *G* (number of particles forming per 100 eV of deposited ionizing energy) and to the local dose rate. Above reactions are included into a set of kinetic equations which define radiolytic behavior of closed gas volume with fixed

temperature. Solutions to the derived set of equations were analyzed and the following key features of radiolysis of steam-hydrogen mixture were established.

1) Molecular hydrogen and hydrogen peroxide are accumulated in gas volume at equal rates which are half as the rate of steam radiolytic decomposition. At temperatures higher ~ 400 °C these rates are proportional to fission rate density in fuel.

2) Formation of hydrogen peroxide is due to recombination of OH radicals. The more OH concentration the more peroxide is formed. As a consequence the peroxide production rate essentially depends on gas mixture composition.

- In steam-rich mixtures it is proportional to steam concentration $c_{\text{H}_2\text{O}}$. This case corresponds to initial stage of fuel oxidation in the intact rod with residual moisture.

- At later oxidation stages with increase of hydrogen fraction in gas mixture OH radicals are consumed in reaction with H_2 molecules. The rate of peroxide generation noticeably diminishes even when $c_{\text{H}_2}/c_{\text{H}_2\text{O}}$ ratio goes close to 0.01. This conclusion is in good agreement with experimental results [11].

Radiolysis-Assisted Fuel Oxidation

Owing to high chemical activity of hydrogen peroxide it can be assumed that all of the H_2O_2 produced by radiolysis is consumed in the fuel oxidation process (see Eq.2) [10]. Under steady-state conditions peroxide flux onto fuel surface equilibrates with its production rate in gas volume. Accordingly, dynamics of fuel stoichiometry obeys the equation

$$c_f \dot{x} = R_T + \dot{c}_{\text{H}_2\text{O}_2} (V_g/V_f). \quad (3)$$

Here c_f and V_f are fuel molar density and volume, respectively, V_g is gas volume adjacent to fuel and the term R_T represents thermal fuel oxidation (it is derived in [15]).

Calculation Results for In-Pile Fuel Oxidation

The above local models were extended to calculate dynamics of gas mixture composition and fuel stoichiometry distribution on the scale of entire fuel rod. For this purpose the fuel rod is divided into separate cells in axial and radial directions. Each fuel cell includes adjacent gas volumes covering cracks, inter-pellet spaces and for central or peripheral cells – central hole or pellet-to-cladding gap. At each time step radiolysis equations are solved for every cell as if it were a closed system. Then fuel oxidation and redistribution of particles in the gas phase are accounted for (primary hydriding calculations with the RTOP code also account for hydrogen uptake by cladding and the hydride growth).

Calculations showed that radiolysis impact on fuel oxidation and hydrogen generation in the intact rod is not noticeable. First, it is related to gradual hydrogen accumulation inside the rod. Even at early oxidation stage, when hydrogen-to-steam content ratio reaches several percent, radiolysis gives a negligible contribution to fuel oxidation. Second, low steam contents typical for the operating intact rods with redundant moisture result in low radiation dose rates (which are proportional to steam concentration) and so – in minor role of radiolysis.

If temperature is decreased, radiolytic effects should become more significant compared to thermal effects as the thermal reactions become slower. Fig.1 shows an example of calculated dynamics of hydrogen generation inside the intact rod with a central hole; fuel is presumed to be homogeneously heated up to $T = 450$ °C. Fission density rate in fuel was taken to be $5 \cdot 10^{18} \text{ m}^{-3}\text{s}^{-1}$ and starting moisture content was 10 ppm. As shown in Fig.1 the initial stage of radiolysis-assisted oxidation is more rapid than out-of-pile thermal oxidation. After somewhat noticeable hydrogen accumulation both calculation results become close. It can be resumed that even at low temperatures typical for pellet-to-cladding gap contribution of radiolysis to fuel oxidation is comparable with that of thermal processes. In hot portions of the fuel rod thermal processes prevail.

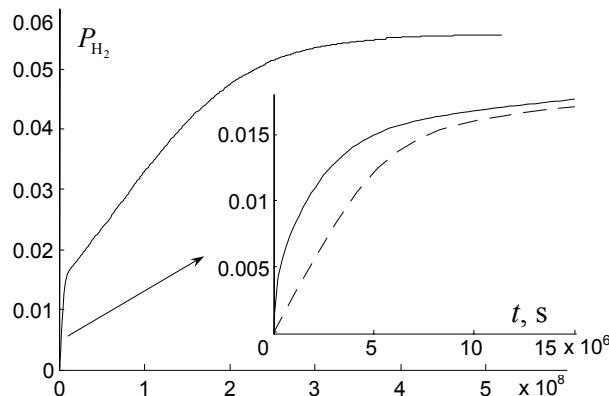


Fig.1. Dynamics of hydrogen partial pressure (MPa) in the intact rod during fuel oxidation at 450 °C; — radiolysis-assisted oxidation, - - - thermal oxidation.

In contrast, radiolysis may play an important role for fuel oxidation and hydrogen generation inside operating defective rods. Total gas pressure in the defective rod may be higher than 15 MPa and the radiation dose rates appear to be orders of magnitude higher than inside the intact rod. Moreover, hydrogen produced due to fuel oxidation is continuously released into coolant. So, decrease of the peroxide generation rate due to hydrogen accumulation is not pronounced. The release rate of gas mixture components into coolant is generally considered to be proportional to their concentrations. The proportionality factor μ lies in the range of 10^{-8} - 10^{-4} s $^{-1}$ [3]. In Fig.2a dynamics of hydrogen partial pressure is calculated for defective rod with $\mu = 10^{-4}$ s $^{-1}$ (large defect) and mean linear power of 20 kW/m. Fig.2b shows the corresponding dynamics of fuel oxidation. (In these calculations fuel pellets have a central hole.)

Under the given conditions for $\sim 10^4$ s helium is released out of the defective rod, so steam pressure goes close to reactor pressure. At the same time hydrogen release out of the rod becomes faster than its generation. It can be seen that hydrogen accumulation due to radiation processes is much more intensive. The peak hydrogen content inside the rod and fuel stoichiometry are greater for the radiolysis-assisted oxidation. Calculated values of stoichiometry deviation are large enough to provide a noticeable change in fuel properties and substantial increase of activity release into coolant.

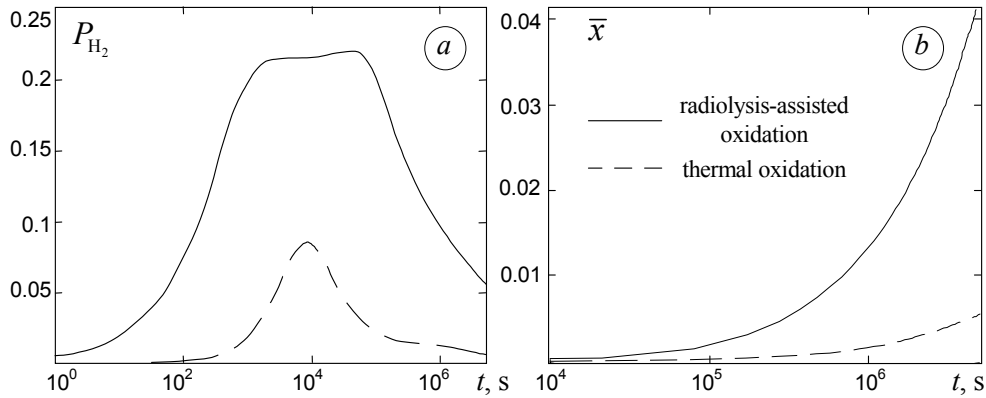


Fig.2. Effect of radiolysis on processes in the defective fuel rod; (a) dynamics of hydrogen generation (MPa); (b) dynamics of mean fuel stoichiometry.

MODEL FOR LOCAL MASSIVE HYDRIDING

The above model is used to calculate hydrogen source inside the operating intact rod which is a key factor in process of cladding primary hydriding. Generated hydrogen is partially adsorbed by cladding and the growing massive hydride consumes the rest.

Modelling of hydrogen adsorption by cladding is based on correlation [16]. This correlation accounts for two mechanisms of hydrogen penetration into metal through the oxide film on cladding inner surface. The first mechanism is hydrogen diffusion through the oxide film and the second one is hydrogen penetration along defects in the oxide. According to [16], permeability of the oxide film at given temperature and hydrogen pressure is governed by its thickness l_{ox} and surface density of atoms initiating linear defects in the oxide, $N_s = 10^{-8}$ - 10^{-4} m $^{-2}$.

Growth of the massive hydride at cladding inner surface is controlled by diffusion transport in zirconium and in the hydride phase. Appropriate growth kinetics commonly obeys the parabolic law. However, experimental observations evidence that major stage of massive hydriding is linear with time [8,17,18]. This fact is attributed to microcracking of hydride layers when they reach a certain thickness l_{cr} . Cracking is possible since specific volume of ZrH $_2$ is 17% higher than that of Zr. Along the formed cracks molecular hydrogen can penetrate to Zr-ZrH $_2$ interface where the new hydride layer starts to grow in metal according to the parabolic law. Grown to thickness l_{cr} the new layer is cracked again and the process goes repeatedly on. Hence, the massive hydride grows in a set of thin successive layers which taken together form the axisymmetric blister (see Figs.4-6). As a whole, the averaged blister growth proves to be linear in time and independent of total size of the hydride. On the base of experimental data [17] it was found that $l_{cr} \approx 0.1$ μ m. It is much less than typical blister sizes. So, growth of each hydride layer can be modeled in 1-D approximation.

The hydride layer thickness is increased according to balance between hydrogen fluxes at the phase interface: between hydrogen incoming through the continuous (without cracks) hydride and hydrogen withdrawal into the metal. The balance equation is

$$M \frac{dl}{dt} = \frac{D_H(T)(y_0 - y_b(t))}{l} - J_{D,n}. \quad (4)$$

Here l is the hydride layer thickness, $M \approx 2 - [y_0 + y_b(t)]/2$ is mean number of H atoms per one Zr atom in the layer, y_0 , y_b are deviations from ZrH $_{2-y}$ stoichiometry at boundaries with zirconium and with the gas phase,

respectively, D_H is hydrogen diffusivity in the hydride, $J_{D,n}$ is diffusion hydrogen flux into cladding in normal direction relative to the hydride layer boundary. Since local conditions (temperature, diffusivities, orientation) for different portions of the growing layer are different, Eq.(4) is solved for each portion separately. The term $J_{D,n}$ in Eq.(4) is found from solution to the thermodiffusion problem in zirconium:

$$\frac{\partial C}{\partial t} + \text{div} \vec{J}_D = 0, \quad \vec{J}_D = -D_{Zr}(T) \left\{ \nabla C + \frac{C Q_H}{N_A k_B T^2} \nabla T \right\}, \quad (5)$$

where C is hydrogen concentration in cladding, D_{Zr} is hydrogen diffusivity in zirconium, $Q_H = 27.2$ kJ/mol is heat of transport, N_A is Avogadro's number, k_B is Boltzmann's constant.

Hydride Initiation

Hydrogen transport in cladding takes place both in radial and axial directions (relative to the hydride). In this process radial diffusion plays an essential role and leads to certain limitations on the hydride initiation stage.

As a starting condition it is presumed that the hydride initiates from some circular inoculating area (free from zirconium oxide) available on cladding inner surface. Note, that processes resulting in crippling of the oxide (dissolution of ZrO_2 in steam-hydrogen atmosphere or PCI) and corresponding incubations times for the hydride initiation are not included into the present model. Growth of the hydride layer at the inoculating site is possible if the right-hand member of Eq.4 is positive. Due to radial diffusion hydrogen withdrawal into cladding $J_{D,n}$ has an order of $D_{Zr} C_0 / R$, where C_0 is terminal hydrogen solubility in zirconium and R is radius of the inoculating area. Clearly, for small enough areas of direct contact between Zr metal and the gas phase, hydrogen inflowing into metal can be rapidly carried away from the surface by diffusion and growth of the massive hydride is inhibited. Critical radius of the inoculating site (R_{cr}) is a sharp decreasing function of temperature. In temperature interval of 300-450 °C it ranges from ~ 250 to $30 \mu\text{m}$.

Hydrogen Transport in Cladding

A rigorous solution to Eqs.(5) at the stage of the blister growth is a complicated computing procedure as hydrogen transport has to be calculated in 2-D area with moving boundary of varying shape. To reduce amount of calculations the problem is solved in the framework of two simplifying assumptions. First, hydrogen diffusion in Zr is regarded as steady state, i.e. at any moment hydrogen distribution conforms to current position and shape of the hydride front. Such an approach is justified since under normal operation conditions typical times of blister growth through the cladding wall of thickness H are appreciably greater than cladding diffusion time H^2/D_{Zr} . Second, radially-averaged hydrogen distribution is calculated using the derived semi-analytical expressions.

Avoiding intricate computations the mentioned assumptions make possible to calculate hydrogen withdrawal from the hydride front into cladding. The calculations take into account radial hydrogen redistribution in Zr, contribution of thermodiffusion and changes in temperature at different portions of the hydride front in course of the blister growth.

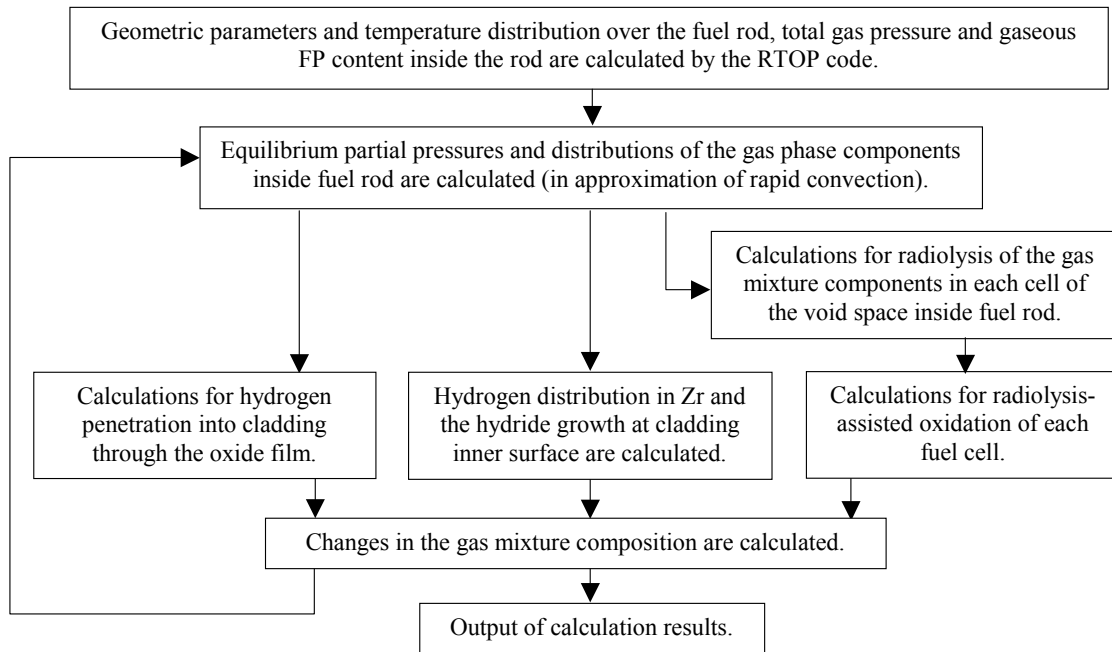


Fig.3. The block diagram for calculations of primary hydriding.

Calculation Results for Primary Massive Hydridding

To provide the self-consistent modelling of primary hydridding the mentioned models were integrated with the RTOP code. This code is dedicated to calculate thermomechanical behavior of a fuel rod with account for the following factors: (i) geometrical parameters of fuel and cladding, (ii) power distribution in fuel, (iii) release of gaseous fission products (FPs), (iv) changes in content and composition of gas mixture inside the rod, (v) dependences of fuel properties on burnup, stoichiometry and temperature. General procedure of primary hydridding calculations is schematically shown in Fig.3.

Growth of the massive hydride was calculated for fuel rods with central hole for different initial levels of residual moisture – in the range of 0.1 up to 10 ppm (by mass). Average linear power for the fuel rod was varied from 10 to 30 kW/m with maximum to average ratio of ~ 1.25 . Sizes of inoculation sites were chosen according to the critical radius R_{cr} . Temperature dependences for model parameters correspond to data from: [19] – for hydrogen diffusivity in zirconium cladding, [20] – for hydrogen diffusivity in zirconium hydride, [21] – for the Sievert's constant, hydrogen solubility limit in zirconium alloys and equilibrium hydride stoichiometry in hydric atmosphere.

Fig.4 shows an example of primary hydridding modelling for fuel rod at linear power of 20 kW/m and initial steam content in fuel of 0.7 ppm. Average cladding temperature in the hydride location was 330 °C, temperature drop over cladding was 30 °C and the oxide film parameters were $l_{ox} = 1 \mu\text{m}$, $N_s = 10^{-8} \text{ m}^{-2}$. The calculated hydride shape is in a qualitative agreement with the shape of massive hydrides observed experimentally [5] (Fig.5). Calculations for higher level of residual moisture in fuel (7 ppm) give the through-cladding hydride (cladding thickness is 650 μm), Fig.6.

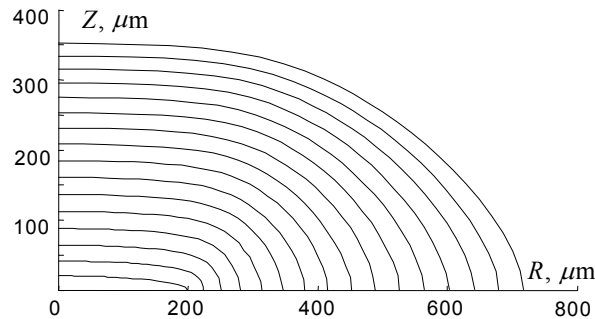


Fig.4. Hydride shape calculated in intervals of 3000 s; moisture content in fuel is 0.7 ppm.

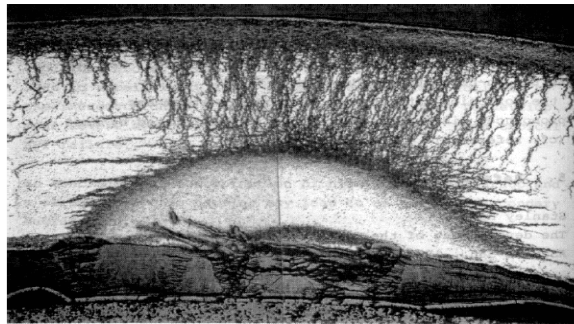


Fig.5. The sunburst shape of the massive hydride observed experimentally [5].

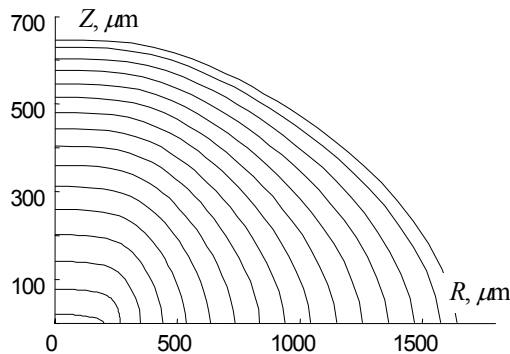


Fig.6. Hydride shape calculated in intervals of 7500 s; moisture content in fuel is 7 ppm.

Test calculations evidence that there are threshold values of initial steam content inside the intact fuel rod which lead to possibility of through-cladding hydride growth and formation of the primary defect. These threshold values are multiparameter functions of such factors as fuel rod geometry, cladding wall material and thickness, oxidation state of cladding inner surface, size of the inoculating area and its location, axial linear power profile in the fuel rod, fuel burnup, coolant temperature and chemistry conditions. Primary failure analysis in each particular case should include the appropriate parameters.

An example of primary hydriding analysis for fresh UO_2 fuel rod with central hole is shown in Fig.7. Fig.7a illustrates the effect of cladding oxidation state on the hydride growth at different linear powers. Moisture content in fuel is set to 7 ppm. As stated above, permeability of the oxide is governed by its thickness l_{ox} and surface density of atoms initiating linear defects N_s . Approximately these parameters come in combination N_s/l_{ox} . The nominal values of N_s/l_{ox} ratio for fresh fuel are expected to be higher than $1\text{-}10\text{ m}^{-3}$. Breakdowns in the manufacturing process may lead to thicker oxide films on cladding inner surface and so, to lower N_s/l_{ox} ratios.

It can be seen in Fig.7a, that low permeability of the oxide leads to hydriding failure. Thinner oxide films provide an efficient hydrogen uptake from the gas phase by cladding. In this case fraction of hydrogen consumed by the hydride is small and its eventual size is small as well. Fig.7b demonstrates the effect of initial moisture content in fuel rod on the hydride eventual size. As shown, the thresholds of hydriding failure depend on power load in fuel rod.

The incubation stage of massive hydriding is not included into modelling at present. For this reason, calculations give only a lower estimate of times necessary for the hydride growth through cladding wall. In fuel rods at average linear power of 30 kW/m this time is found to have the order of 12 hours, at 20 kW/m – about a day and at 10 kW/m the corresponding time is approximately three days.

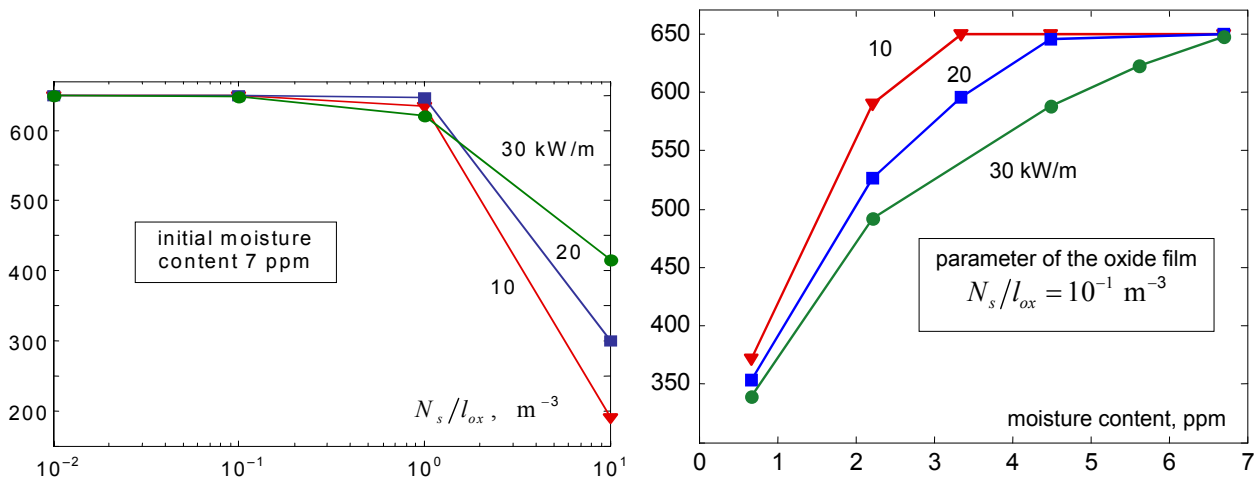


Fig.7. Depth of the hydride penetration into cladding (μm) as a function of (a) cladding oxidation level, (b) initial moisture content in fuel. Average linear power θ – 10 kW/m, \square – 20 kW/m, \star – 30 kW/m.

CONCLUSION

New models were developed to describe the process of primary hydriding in zirconium claddings of operating intact rods with residual moisture.

- The model for radiolysis of steam-hydrogen mixture accounts for effects of temperature, pressure, mixture composition, fuel geometry and radiation conditions inside fuel rod.
- The model for radiolysis-assisted fuel oxidation describes kinetics of UO_2 oxidation under in-pile conditions and allows to calculate dynamics of hydrogen generation inside operating fuel rod.
- The 2-D model for growth of the massive hydride at cladding inner surface takes into account hydrogen withdrawal into cladding and effect of thermodiffusion. The model allows to reproduce the hydride shape observed experimentally.

Integrated into the RTOP code these models provide the self-consistent description of physical processes relevant to primary massive hydriding. The analysis of the calculation results shows that there are threshold values of initial steam content inside intact fuel rod which make possible the through-cladding hydride growth. These threshold values depend on oxidation level of cladding inner surface, axial linear power profile in the fuel rod, fuel rod geometry, cladding temperature conditions and hydrogen diffusivities in zirconium and zirconium hydride. Given the initial parameters, the code allows to calculate sizes of the grown massive hydrides. Lower estimates of growth times can be

obtained as well. The code can be also used to analyze different scenarios of hydriding rod failures under various operation conditions and to form the fuel rod failure criteria.

ACKNOWLEDGEMENTS

The reported investigation was carried out under the contract with the Joint Stock Company "TVEL", Russia, and was partially supported by the Russian Foundation for Basic Research, project No.02-02-16494.

REFERENCES

1. Parrat, D., Genin, J.B., Musante, Y., Petit, C. and Harrer, A., "Failed Rod Diagnosis and Primary Circuit Contamination Level Determination Thanks to the DIADEME Code". *IAEA Technical Meeting on Fuel Failures in Water Reactors: Causes and Mitigation*, Bratislava, June 17 - 21, 2002.
2. Koo, Y.-H., Sohn, D.-S. and Yoon, Y.-Ku, "An Analysis Method for the Fuel Rod Gap Inventory of Unstable Fission Products During Steady-State Operation", *J. Nucl. Mater.*, Vol. 209, 1994, pp. 62-78.
3. Lewis, B.J., "A Generalized Model for Fission-Product Transport in the Fuel-Sheath Gap of Defective Fuel Elements", *J. Nucl. Mater.*, Vol. 175, 1990, pp. 218-226.
4. Kim, Y., Lee, M., Kim, K. *et al.*, "Hydriding Failure Analysis Based on PIE Data", *Proc. Intern. Topical Meeting "LWR Fuel Performance"*, Park City, Utah, USA, April 10-13, 2000.
5. Edsinger, K., "A Review of Fuel Degradation in BWR", *Proc. Intern. Topical Meeting "LWR Fuel Performance"*, Park City, Utah, USA, April 10-13, 2000.
6. Garzarolli, R. von Jan and Stehle, H., "The Main Causes of Fuel Element Failure in Water-Cooled Power Reactors", *Atomic Energy Review*, 17 1, 1979.
7. "Review of Fuel Failures in Water Cooled Reactors", *IAEA Report*, Technical Report Series No.388, IAEA, Vienna, 1998.
8. Kim, Y.S., Wang, W.E., Olander, D.R. and Yagnik, S.K., "High Pressure Hydriding of Sponge-Zr in Steam-Hydrogen Mixtures", *J. Nucl. Mater.*, Vol. 246, 1977, pp. 43-52.
9. Dobrov, B.V., Kanukova, V.D., Khoruzhii, O.V., Kourchatov, S.Yu., Likhanskii, V.V. and Sakharov B.B., "The Development of a Mechanistic Code on Fission Product Behavior in the Polycrystalline UO₂ Fuel," *Nucl. Eng. and Design*, Vol. 195 (3), 2000, pp. 361-371.
10. Lewis, B.J., Szpunar, B. and Iglesias, F.C., "Fuel Oxidation and Thermal Conductivity Model for Operating Defective Fuel Rods," *J. Nucl. Mat.*, Vol. 306, 2002, pp. 30-43.
11. Olander, D.R. *et al.*, "Chemical Processes in Defective LWR Fuel Rods," *J. Nucl. Mater.*, Vol. 248, 1997, pp. 214-219.
12. Byakov, V.M. and Nichiporov, F.G., *Radiolysis of Water in Nuclear Reactors*, Moscow, 1990 (*in Russian*).
13. Pickaev, A.K., *Modern Radiation Chemistry. Radiolysis of Gases and Liquids*, Moscow, 1986 (*in Russian*).
14. *The NIST Chemical Kinetics Database*, NIST Standard Reference Database 17-2Q98, 1998.
15. Dobrov, B.V., Likhanskii, V.V., Ozrin, V.D., *et al.*, "Kinetics of UO₂ Oxidation in Steam Atmosphere", *J. Nucl. Mater.*, Vol. 255, 1998, pp. 59-66.
16. Smith, T., "Kinetics and Mechanism of Hydrogen Permeation of Oxide Films on Zirconium", *J. Nucl. Mater.*, Vol. 18, 1966, pp. 323-336.
17. Meyer, G., Kobrinsky, M., Abriata, J.P. and Bolcich, J.C., "Hydriding Kinetics of Zircaloy-4 in Hydrogen Gas", *J. Nucl. Mater.*, Vol. 229, 1996, pp. 48-56.
18. Kim, Y.S. and Kim, S.K., "Kinetic Studies on Massive Hydriding of Commercial Zirconium Alloy Tubing," *J. Nucl. Mater.*, Vol. 270, 1999, pp. 147-153.
19. Shmakov, A.A., Bibilashvilly, Yu.K., Kalin, B.A. and Smirnov E.A., *Prediction of Possibility of Hydride Cracking in Zirconium Claddings of Fuel Rods*, MEPhI Preprint 003-99, 1999 (*in Russian*).
20. Andrievskii, R.A., *The Metallurgy of Hydrides*, Moscow, Metallurgy, 1986, (*in Russian*).
21. Douglass D.L., "The Metallurgy of Zirconium", *Atomic Energy Review*, IAEA -Vienna, 1971.